SLAC-PUB-666
September 1969
(EXP)

STUDY OF THE REACTION $\gamma p \rightarrow \pi^+\pi^-\pi^+\pi^- p$ ABOVE 4.5 GEV AND EVIDENCE FOR A πA_1 ENHANCEMENT*

M. Davier,** I. Derado,*** D. C. Fries,† F. F. Liu,
R. F. Mozley, A. Odian, J. Park, W. P. Swanson, F. Villa, and D. Yount††

Stanford Linear Accelerator Center
Stanford University, Stanford, California 94305

ABSTRACT

We have studied the reaction $\gamma p \rightarrow \pi^+\pi^-\pi^+\pi^- p$ between 4.5 and 18 GeV. About 75% of these events contain the resonances Δ^{++} and ρ^0. Evidence is presented for a πA_1 enhancement with $M = 1.55 \pm 0.04$ GeV and $\Gamma = 0.26 \pm 0.11$ GeV. Comparison is made with the $\pi^+\pi^-$ mass distribution in the reaction $\gamma p \rightarrow \pi^+\pi^- p$.

(Submitted to the International Symposium on Electron and Photon Interactions at High Energies, Daresbury, September 1969.)

*Work supported by the U.S. Atomic Energy Commission.

**Now at Laboratoire de l'Accelerateur Lineaire, Orsay France.

***Now at Max Planck Institut f. Physik and Astrophysik, Munich, Germany.

†Now at Kernforschungs Zentrum, Karlsruhe, Germany.

††Now at University of Hawaii, Honolulu, Hawaii.

In a multibody photoproduction experiment done with the 2.2-meter SLAC streamer chamber in an 18 GeV bremsstrahlung beam, 663 events of the type:

$$\gamma p \rightarrow \pi^+\pi^-\pi^+\pi^- p \tag{1}$$

have been measured and analyzed. The geometrical and kinematical analysis is described elsewhere.[1]

Reaction (1) is interesting as it could reveal the existence of new vector mesons of higher mass decaying into 4π rather than into 2π. In order to study this problem we selected 518 events with photon energies above 4.5 GeV. About 75% of reaction (1) goes into well-known resonances; we observe the following channels:

$$\gamma p \rightarrow \pi^+\pi^-\pi^-\Delta^{++} \tag{2}$$

$$\gamma p \rightarrow \pi^+\pi^-\rho^0 p \tag{3}$$

$$\gamma p \rightarrow \pi^-\rho^0\Delta^{++} \tag{4}$$

$$\gamma p \rightarrow A_1^{\pm}\pi^{\mp} p \tag{5}$$

To obtain cross sections we fitted each channel with an incoherent superposition of peripheral phase-space[2] and a Breit-Wigner form for the resonance.[3] For the Δ^{++} and ρ^0 we used:

$$BW(m) = \frac{m}{q} \frac{\Gamma(m)}{\left(m^2 - m_0^2\right)^2 + m^2\Gamma^2(m)}$$

$$\Gamma(m) = \Gamma_0 \left(\frac{q}{q_0}\right)^3 R$$

where $q(q_0)$ is the center-of-mass momentum at the mass $m(m_0)$ and

$$R = \frac{2.2\, m_\pi^2 + q_0^2}{2.2\, m_\pi^2 + q^2} \qquad \text{for } \Delta^{++}$$

$$R = \frac{2q_0^2}{q_0^2 + q^2} \qquad \text{for } \rho^o$$

The experimental data and fitted curves are shown in Fig. 1 and Fig. 2a, b; the corresponding cross sections are given in Table 1.

$\underline{\gamma p \rightarrow \pi^+ \pi^- \pi^- \Delta^{++}}$

The 3π mass plot in the reaction $\gamma p \rightarrow \pi^+ \pi^- \pi^- \Delta^{++}$ does not show any significant structure in the A_1 and A_2 mass region. The reaction $\gamma p \rightarrow A_2^- \Delta^{++}$ has been observed at 5.25 GeV, with a cross section of $0.7 \pm 0.3\ \mu b$.[4] From our data we can set a limit of $0.2\ \mu b$ averaged between 4.5 and 18 GeV.

$\underline{\gamma p \rightarrow \pi^- \rho^o \Delta^{++}}$

We have also studied the systematics of the quasi-three-body reaction (4). At these high energies one might expect diffraction dissociation producing high-mass isobars decaying into $\pi\Delta$:

$$\gamma p \rightarrow \rho^o\, N^*_{I=\frac{1}{2}} \qquad (6)$$
$$\quad \hookrightarrow \pi^- \Delta^{++}$$
$$\quad \hookrightarrow \pi^+ \Delta^o$$

Since we do not observe Δ^o production, we can state that not more than 30% of reaction (4) proceeds through this type of diffraction dissociation.

To study the possibility of other mechanisms, we displayed our data in a longitudinal phase-space diagram.[5] Figure 3a shows the polar diagram of longitudinal center-of-mass momenta and Fig. 3b shows the radial projection. The striking effect is the accumulation of events in the region where π^- has a small longitudinal momentum and $\rho^o(\Delta^{++})$ a large forward (backward) longitudinal momentum. The plot indicates that the π^- is connected with the Δ^{++} in less than 20% of the cases, and thus is consistent with the 30% limit mentioned above.

The momentum transfer distributions fitted to the form $Ae^{-B|t-t_{min}|}$ give the following numbers:

$B = 6.7 \pm 1.5\ GeV^{-2}$ proton to Δ^{++}

$B = 3.7 \pm 0.4\ GeV^{-2}$ photon to ρ^o

$B = 1.0 \pm 0.4\ GeV^{-2}$ photon to π^-

$\gamma p \rightarrow \pi^+\pi^-\pi^+\pi^- p$

The unselected 4π mass plot shows no significant structure apart from a possible excess near 1.5 GeV mass (Fig. 4a). This shoulder is enhanced when events which contain a Δ^{++} are removed ($1.16 < M_{(p\pi^+)} < 1.32$ GeV). This is to be expected if the effect is connected with the 4π above (Fig. 4b); it should be noticed that the Δ^{++} cut does not distort the 4π mass phase space appreciably because the background under the Δ^{++} peak (see Fig. 1) is small.

With the same Δ^{++} cut, the 3π mass spectrum shows a pronounced peak near the A_1 mass (Fig. 5a); this peak is enhanced by requiring that two of the 3π are in the ρ^o mass band (Fig. 5b). A less significant peak is seen at the A_2 mass. Although the former peak has not yet been studied in detail, we tentatively identify it as the A_1 because of its mass and apparent $\rho\pi$ decay.

In order to determine where the A_1 signal came from, we studied the 3π mass spectrum for different 4π mass regions (Fig. 6a, b, c). A strong A_1 peak appears when the 4π mass lies between 1.4 and 1.8 GeV. This selection of $M(4\pi)$ appears to contain all A_1 observed in our sample. On the plot containing both positive and negative 3π combinations, the width of the A_1 appears broader than the accepted value. In Fig. 7, where the positive and negative combinations are plotted separately, we see that each charge state has a width consistent with 80 MeV, but the masses are shifted relative to each other. This shift would seem to account for the apparently large width. The mass of the peak of the combined plot (Fig. 4c), is about 1115 MeV. Figure 4c represents the 4π mass plot with the 3π mass in the A_1 band (1.015 - 1.215 GeV) and shows evidence for a broad peak.

To understand the background and possible reflections through the various cuts, we generated Monte-Carlo events according to the reactions (1), (2), (3), (4) and (5), using observed momentum transfer distributions. The Monte-Carlo distributions fit the experimental plots well (Figs. 1, 2, 4, 5, 6) so that we feel confident that we understand the background in the 4π spectrum. Furthermore, this background describes the data well when cuts are made in control regions, below and above the A_1. Assuming that the enhancement corresponds to a single resonance, the fitted mass and width are:

$$M = 1.55 \pm 0.04 \text{ GeV}$$

$$\Gamma = 0.26 \pm 0.11 \text{ GeV}$$

In Table 2 we show results of fitting the momentum transfer distributions from the photon to the A_1 and to the 4π enhancement. We also give the forward-backward asymmetry of π and A_1 in the πA_1 helicity frame which is consistent with uniformity.

To see if the same effect is present in 2π decay, we consider the reaction

$$\gamma p \rightarrow \pi^+ \pi^- p \qquad (7)$$

Figure 8 shows the $\pi^+\pi^-$ mass plot where we combine our data together with DESY[6] and SLAC[4] bubble chamber data above 5 GeV. An enhancement similar to the one observed in the πA_1 channel, although less significant, is observed with the following parameters:

$$M = 1.54 \pm 0.02 \text{ GeV}$$

$$\Gamma = 0.24 \pm 0.08 \text{ GeV}$$

If we examine lower energy data at 4.3 GeV[7] and recently available data at 4.7 GeV[8] no effect is observed; however, problems of Δ^{++} reflection are more severe in the lower energy region.

If we were to interpret the two effects as coming from the same resonance, we find the following branching ratios:

$\pi^+\pi^-$	0.6 ± 0.25
πA_1	0.4 ± 0.25

giving a cross section for both channels of 1.1 ± 0.5 μb.

The Veneziano model[9] predicts the existence of new I=1 vector mesons at masses around 1.25 (ρ') and 1.65 GeV (ρ''). If we fix the ρ' mass at 1.25 GeV, we can derive from our data an upper limit of the cross section

$$\sigma(\gamma p \to \rho' p), \quad \rho' \to \pi^+\pi^-$$

as a function of the total width $\Gamma_{\rho'}$ (Fig. 9). It is worth mentioning that $\Gamma_{\rho'}$ might be as large as a few hundred MeV, due to a large πA_1 decay width.[10]

It is not easy to interpret our 1.55 GeV enhancement in the present Veneziano scheme, both because of the mass and of the decay width in 2π.

ACKNOWLEDGEMENTS

The work reported here was participated in by a large number of people other than those mentioned on the title page. In particular, L. Schwarcz directed many phases of the construction. Among those whose help has also been of great value are the following: M. Aleksandrov, D. Blanchard, B. Boyd, J. Brandt, R. Chamberlin, R. Ching, N. Cooper, D. Danielson, H. Ebrahimi, B. Hirsch, D. Lebet, V. Lee, R. Leedy, E. Maninger, D. Maue, E. McNerney, A. Omahen, F. Plunder, T. Pulliam, W. Quiett, P. Saunders, M. Schlesinger, G. Schultz, F. Shuster, J. Siebe, G. Tao, P. Thingstad, W. Wadley, and S. Weller.

In addition it is a pleasure to thank the accelerator and computer operating groups and the machine shops for their assistance.

REFERENCE AND NOTES

1. M. Davier, I. Derado, D. Drickey, D. Fries, R. Mozley, A. Odian, F. Villa, and D. Yount, Report No. SLAC-PUB-613, Stanford Linear Accelerator Center, Stanford University, Stanford, California (1969) (to be published).

2. Observed t distributions were used in generating the background curves.

3. J. D. Jackson, Nuovo Cimento 34, 1644 (1964).

4. J. Ballam et al., Report No. SLAC-PUB-625, Stanford Linear Accelerator Center, Stanford University, Stanford, California (1969).

5. L. Van Hove, Phys. Letters 28B, 429 (1969).

6. A.B.B.H.H.M. Collaboration, Phys. Rev. 175, 1669 (1968).

7. Y. Eisenberg et al., Phys. Rev. Letters 22, 699 (1969).

8. SLAC, Tufts, U.C., Berkeley Collaboration, submitted to the International Symposium on Electron and Photon Interactions at High Energies, Daresbury (1969).

9. G. Veneziano, Nuovo Cimento 57A, 190 (1968); and private communication.

10. P. H. Frampton, Stanford Linear Accelerator Center, Stanford University, Stanford, California, private communication.

TABLE 1

CROSS SECTIONS FOR VARIOUS CHANNELS

Channel	$4 < E\gamma < 8$ GeV $\sigma(\mu b)$	$8 < E\gamma < 18$ GeV $\sigma(\mu b)$
$\gamma p \rightarrow \pi^+\pi^-\pi^-\Delta^{++}$	1.4 ± 0.5	1.0 ± 0.2
$\rho^o\pi^+\pi^- p$	1.3 ± 0.6	0.5 ± 0.2
$\rho^o\pi^-\Delta^{++}$	1.4 ± 0.4	0.32 ± 0.08

These cross sections are the result of a preliminary analysis. An additional 20% uncertainty in absolute value of all channels may exist.

TABLE 2

Momentum transfer distribution fitted to $A\ e^{-B|t-t_{min}|}$.

B (GeV^2)

Photon to 3π system	
A_1	Background
1.7 ± 0.3	2.6 ± 0.2

Photon to 4π system	
πA_1	Background
5.8 ± 0.4	3.8 ± 0.1

Forward-backward asymmetry in πA_1 helicity system.

πA_1	Background
-0.06 ± 0.12	+0.30 ± 0.14

LIST OF FIGURES

8. 2π mass distribution in reaction $\gamma p \to \pi^+ \pi^- p$

DESY, 127 events[6] $5 < E\gamma < 5.8$ GeV

SLAC HBC, 538 events[7] $E\gamma = 5.25$ GeV

SLAC streamer chamber (this experiment), 968 events $4.5 < E\gamma < 18$ GeV.

9. Upper limit on $\sigma(\gamma p \to \rho' p)$ for $M(\rho') = 1.25$ GeV as a function of $\Gamma_{\rho'}$.

($4.5 < E\gamma < 18$ GeV).

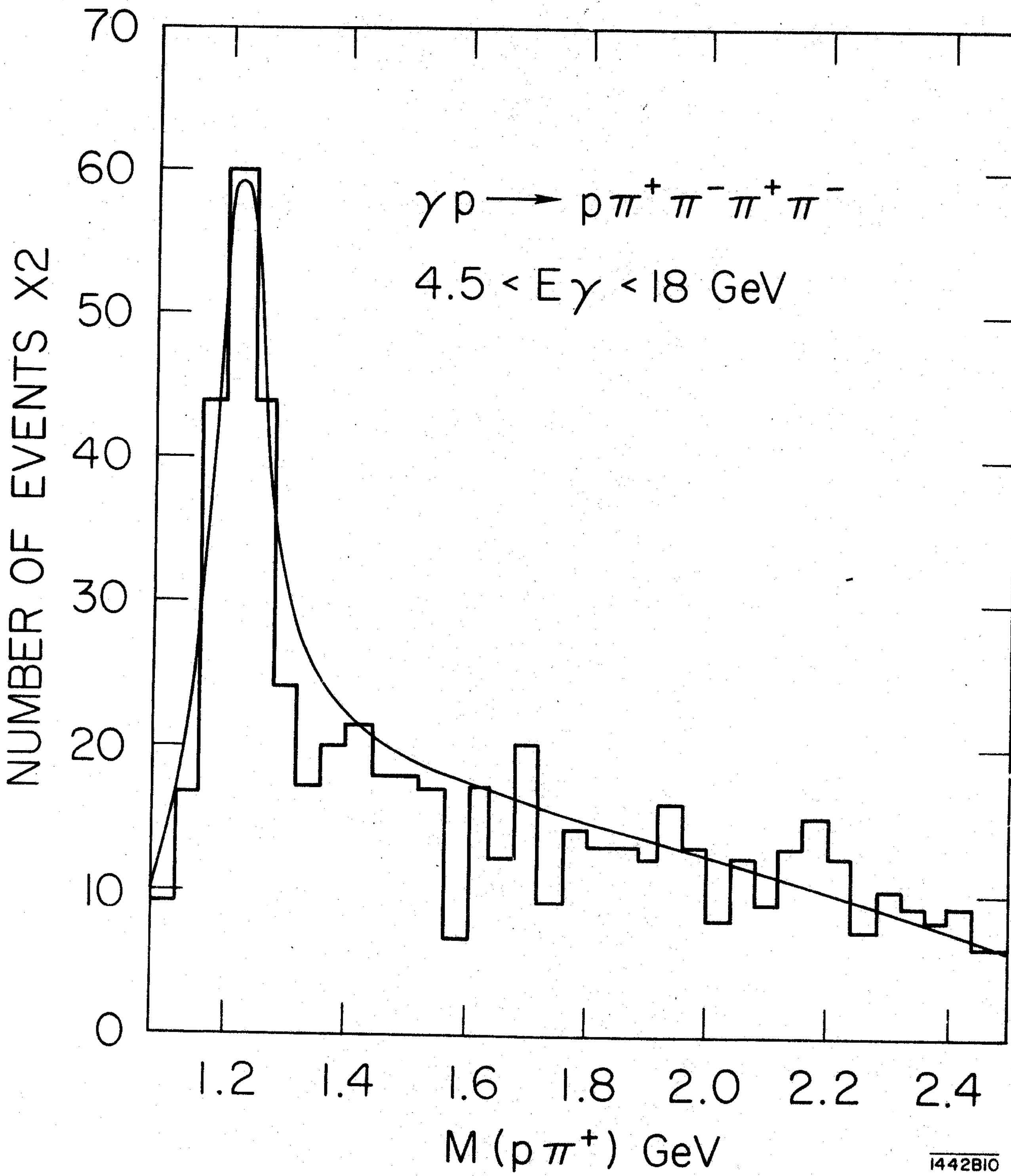

NUMBER OF EVENTS X2
0
10
20
30
40
50
60
70
$\gamma p \longrightarrow p\pi^+\pi^-\pi^+\pi^-$
$4.5 < E\gamma < 18$ GeV
1.2
1.4
1.6
1.8
2.0
2.2
2.4
$M(p\pi^+)$ GeV
1442B10

Fig. 1

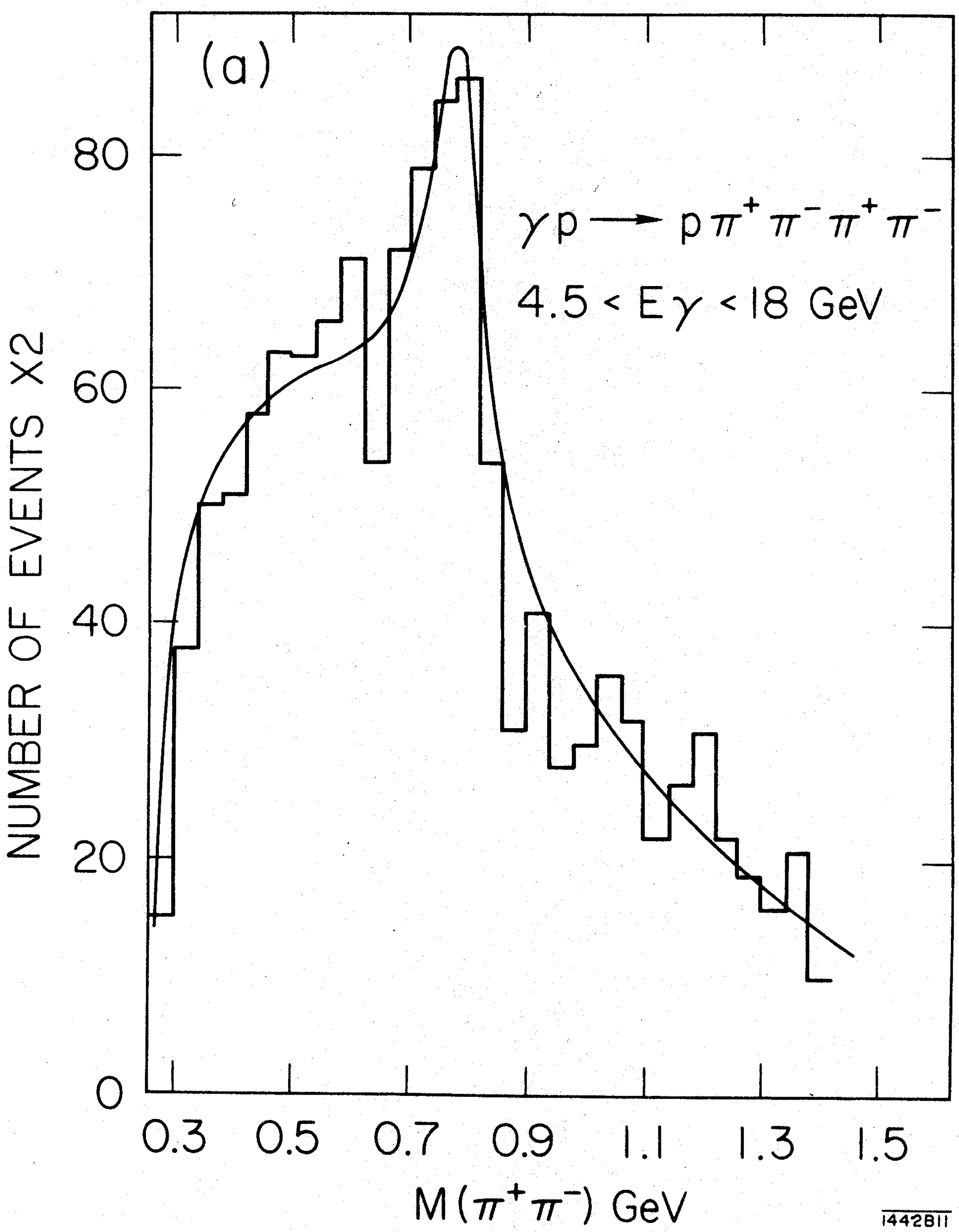

(a)
80
60
40
20
0
NUMBER OF EVENTS X2
γp ⟶ pπ⁺π⁻π⁺π⁻
4.5 < Eγ < 18 GeV
0.3
0.5
0.7
0.9
1.1
1.3
1.5
M(π⁺π⁻) GeV
1442B11

Fig. 2a

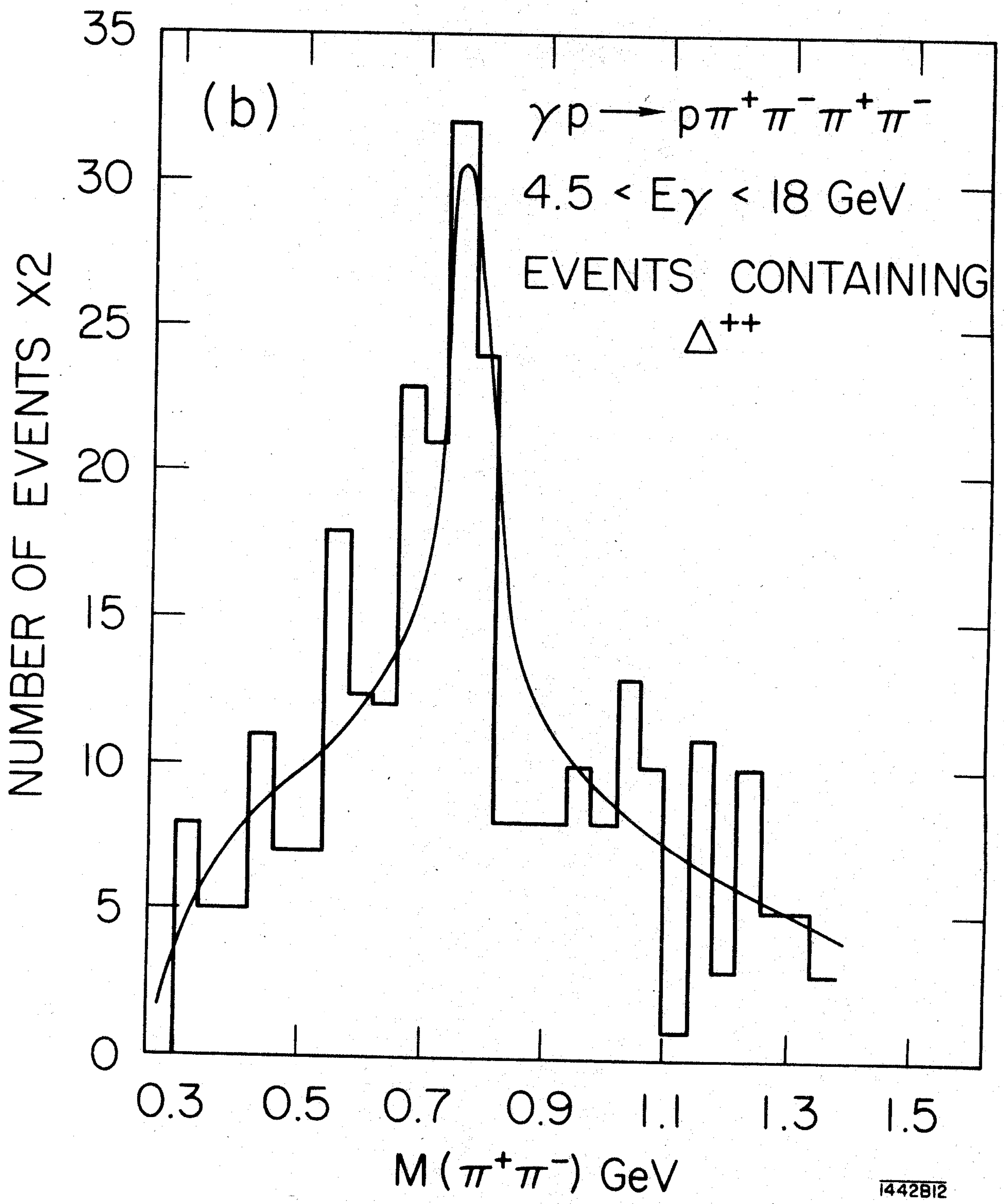
(b)
$\gamma p \rightarrow p\pi^+\pi^-\pi^+\pi^-$
$4.5 < E\gamma < 18$ GeV
EVENTS CONTAINING
Δ^{++}
NUMBER OF EVENTS X2
0
5
10
15
20
25
30
35
0.3
0.5
0.7
0.9
1.1
1.3
1.5
$M(\pi^+\pi^-)$ GeV
1442B12

Fig. 2b

$\gamma p \rightarrow \rho^{\circ} \pi^{-} \Delta^{++}$

$4.5 < E\gamma < 18$ GeV

LONGITUDINAL MOMENTA $\frac{P_L}{P_\gamma}$

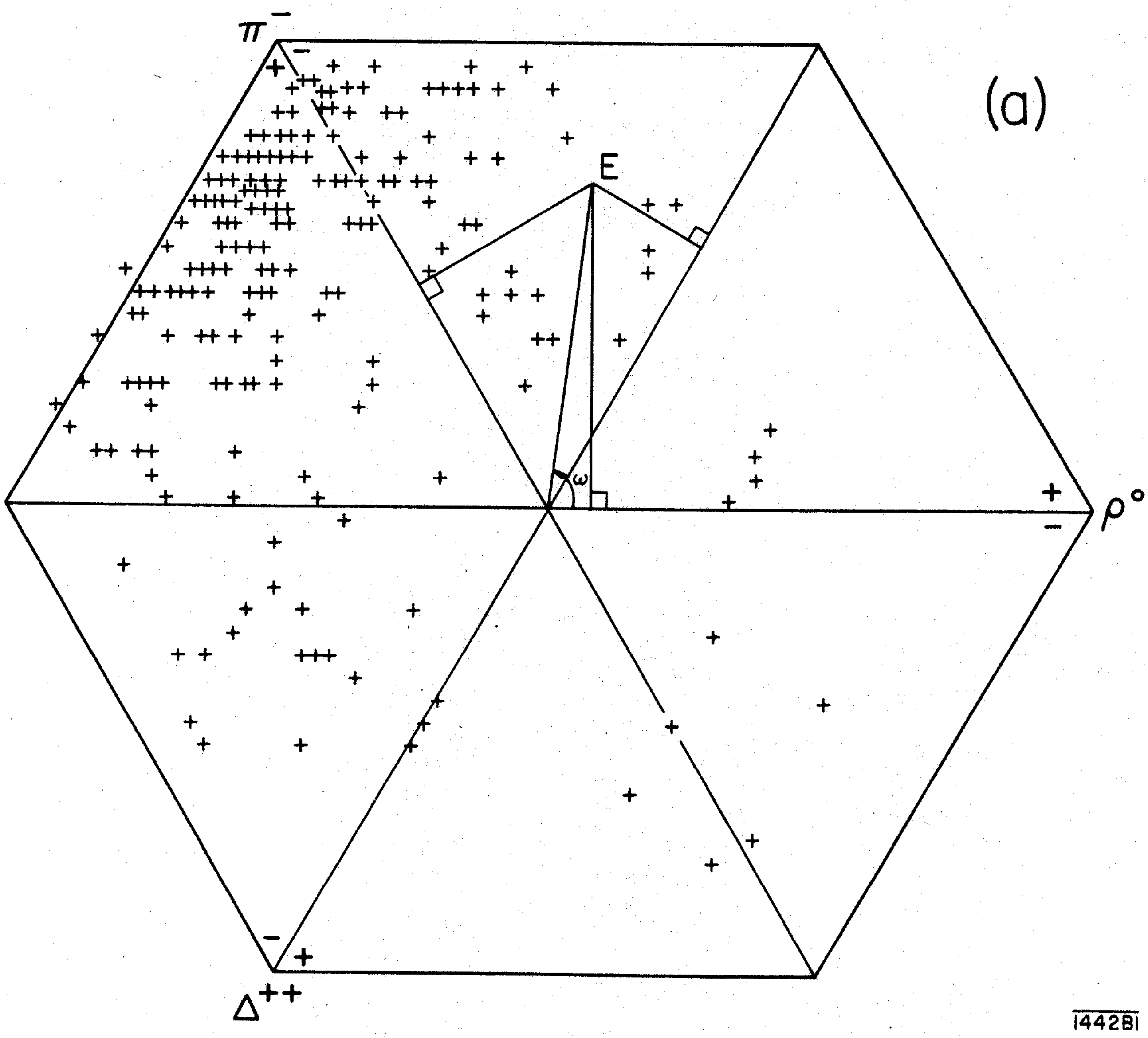

Fig. 3a

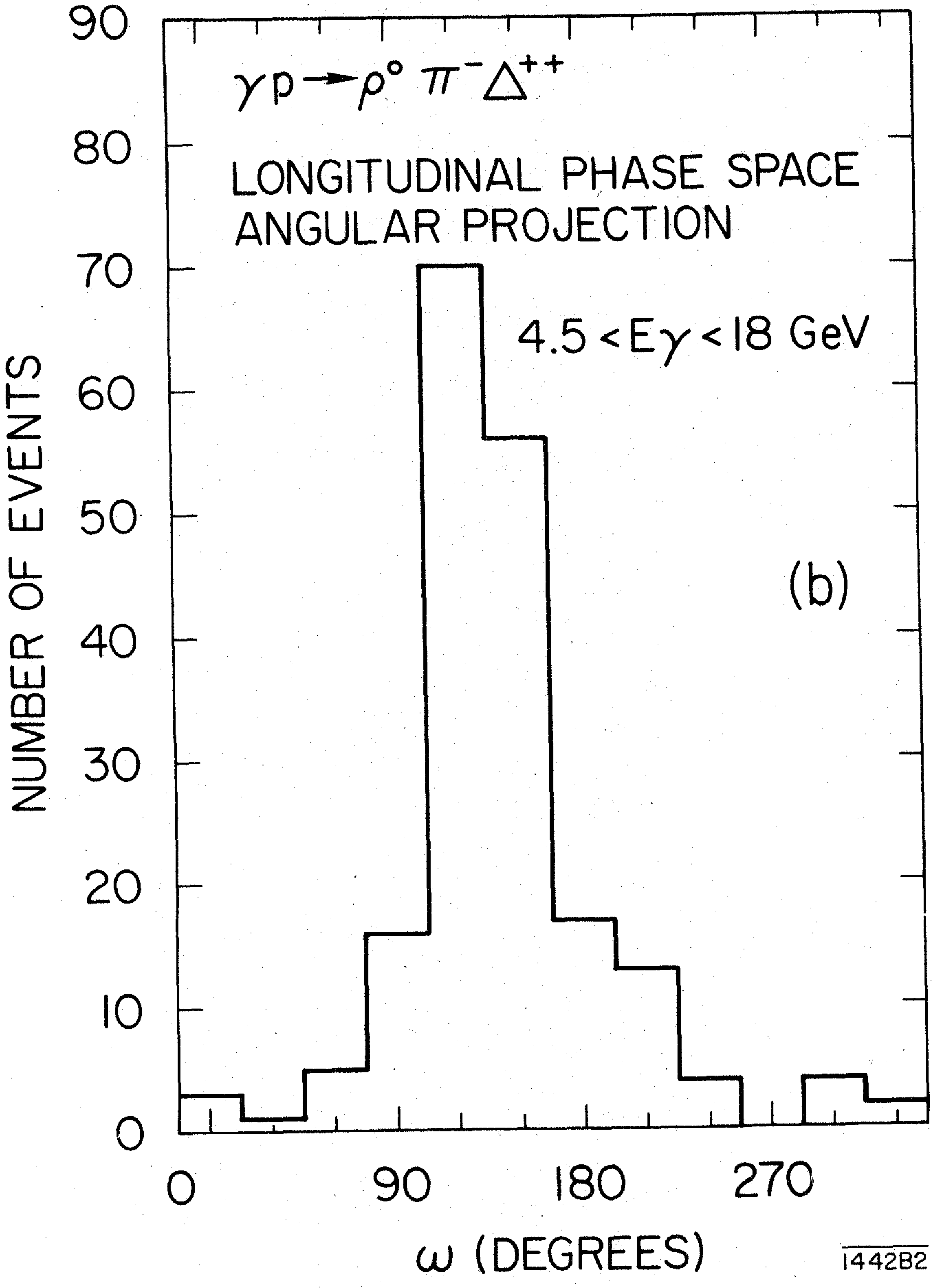

$\gamma p \to \rho^0 \pi^- \Delta^{++}$
LONGITUDINAL PHASE SPACE
ANGULAR PROJECTION
$4.5 < E\gamma < 18$ GeV
(b)
NUMBER OF EVENTS
0
10
20
30
40
50
60
70
80
90
0
90
180
270
ω (DEGREES)
1442B2

Fig. 3b

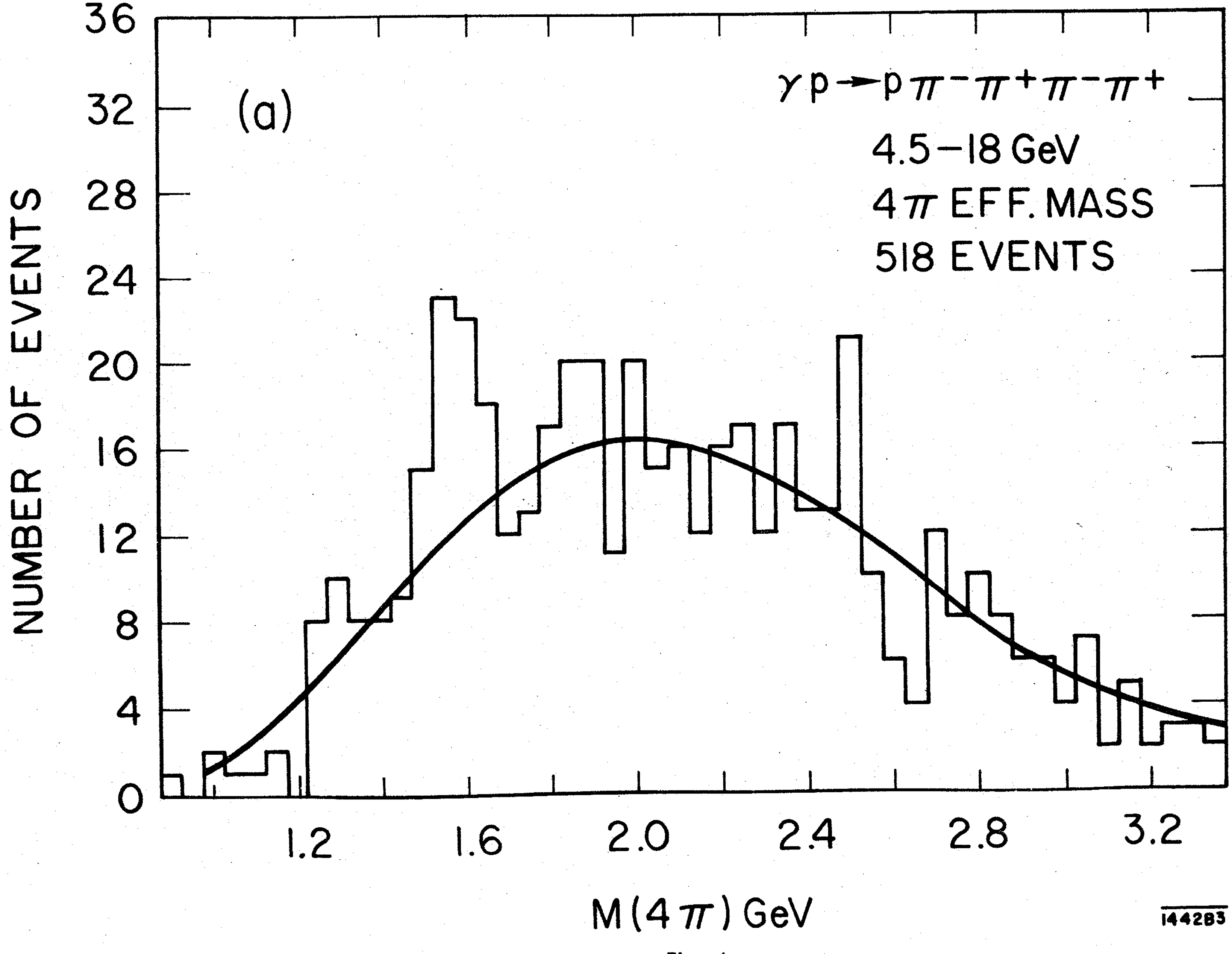
NUMBER OF EVENTS
36
32
28
24
20
16
12
8
4
0
(a)
γp → pπ⁻π⁺π⁻π⁺
4.5–18 GeV
4π EFF. MASS
518 EVENTS
1.2
1.6
2.0
2.4
2.8
3.2
M(4π) GeV
144283

Fig. 4a

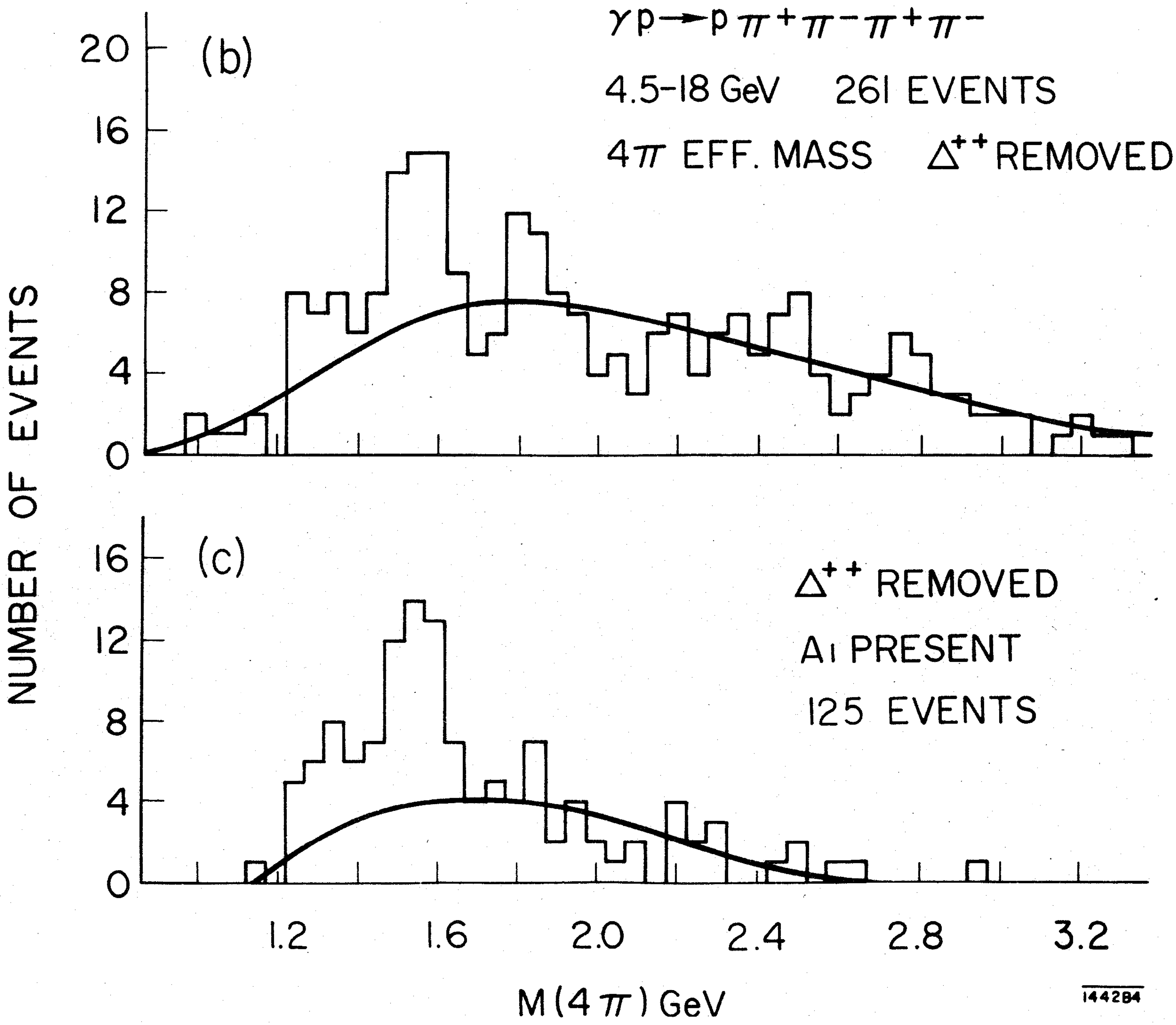
γp → pπ⁺π⁻π⁺π⁻
(b)
4.5–18 GeV 261 EVENTS
4π EFF. MASS Δ⁺⁺ REMOVED
(c)
Δ⁺⁺ REMOVED
A1 PRESENT
125 EVENTS
NUMBER OF EVENTS
M(4π) GeV
0
4
8
12
16
20
1.2
1.6
2.0
2.4
2.8
3.2
1442B4

Fig. 4b,c

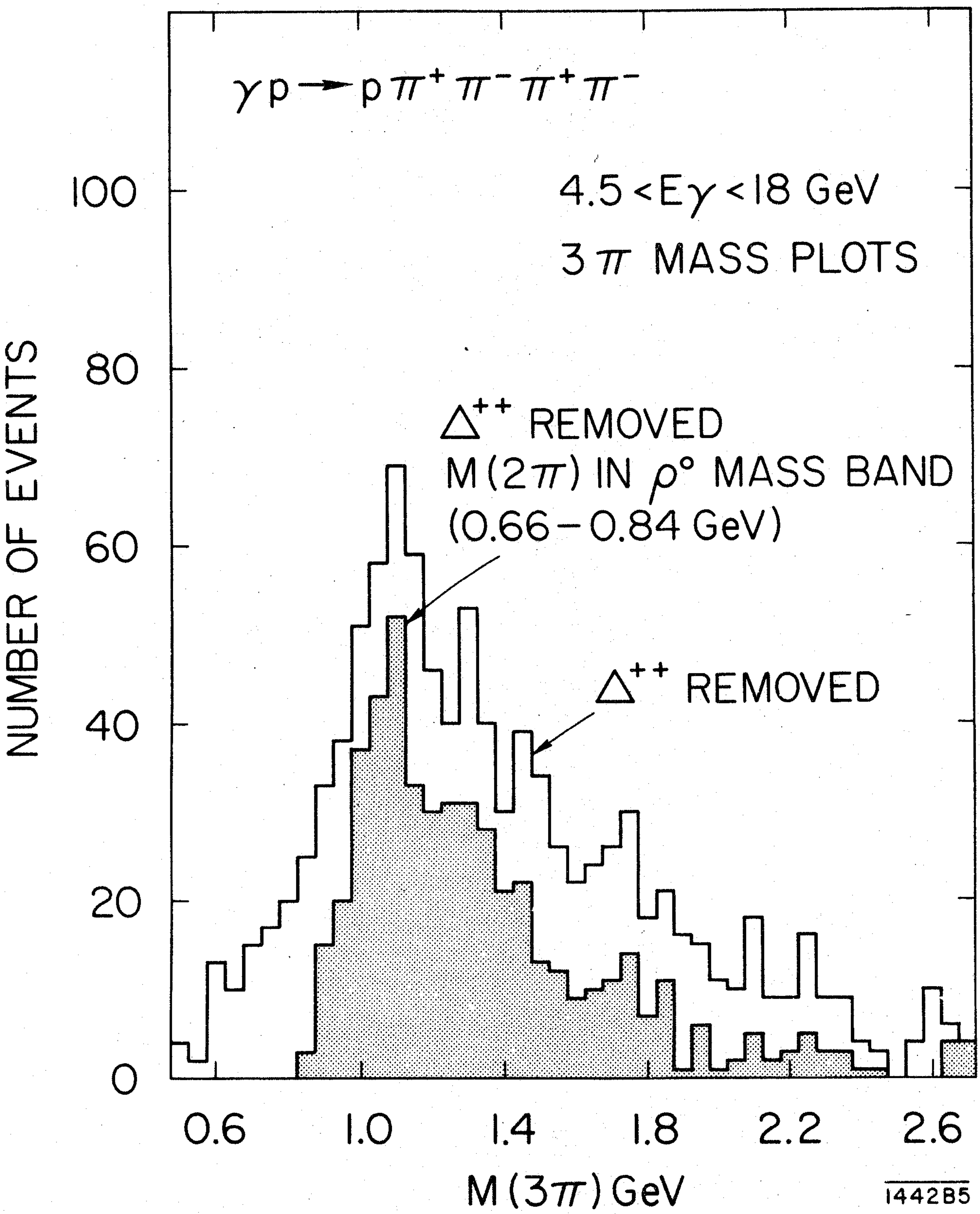

$\gamma p \rightarrow p\pi^+\pi^-\pi^+\pi^-$
4.5 < Eγ < 18 GeV
3π MASS PLOTS
Δ++ REMOVED
M(2π) IN ρ° MASS BAND
(0.66–0.84 GeV)
Δ++ REMOVED
NUMBER OF EVENTS
0
20
40
60
80
100
0.6
1.0
1.4
1.8
2.2
2.6
M(3π) GeV
1442B5

Fig. 5a,b

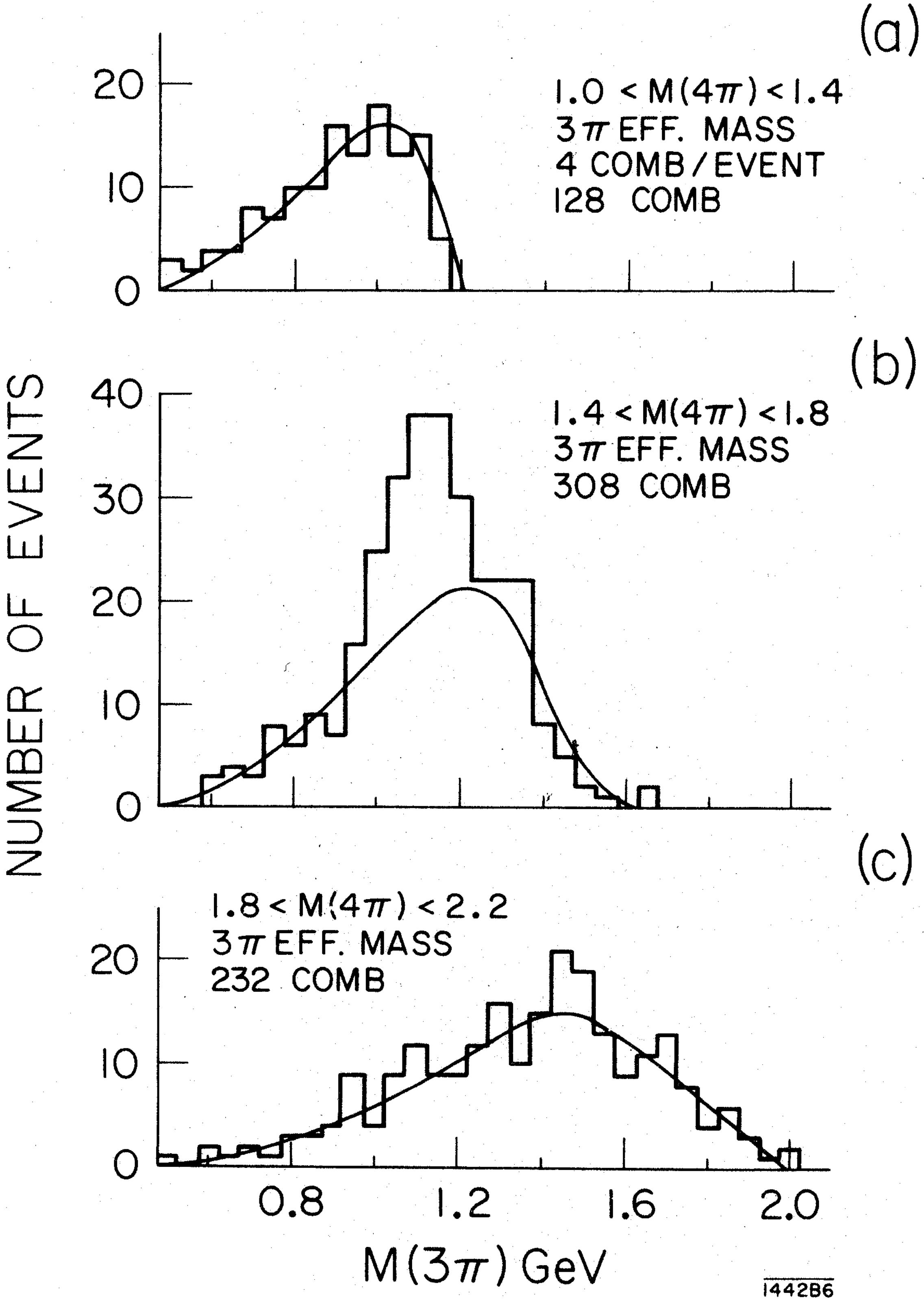

(a)
1.0 < M(4π) < 1.4
3π EFF. MASS
4 COMB / EVENT
128 COMB
(b)
1.4 < M(4π) < 1.8
3π EFF. MASS
308 COMB
(c)
1.8 < M(4π) < 2.2
3π EFF. MASS
232 COMB
NUMBER OF EVENTS
0
10
20
30
40
0.8
1.2
1.6
2.0
M(3π) GeV
144286

Fig. 6a,b,c

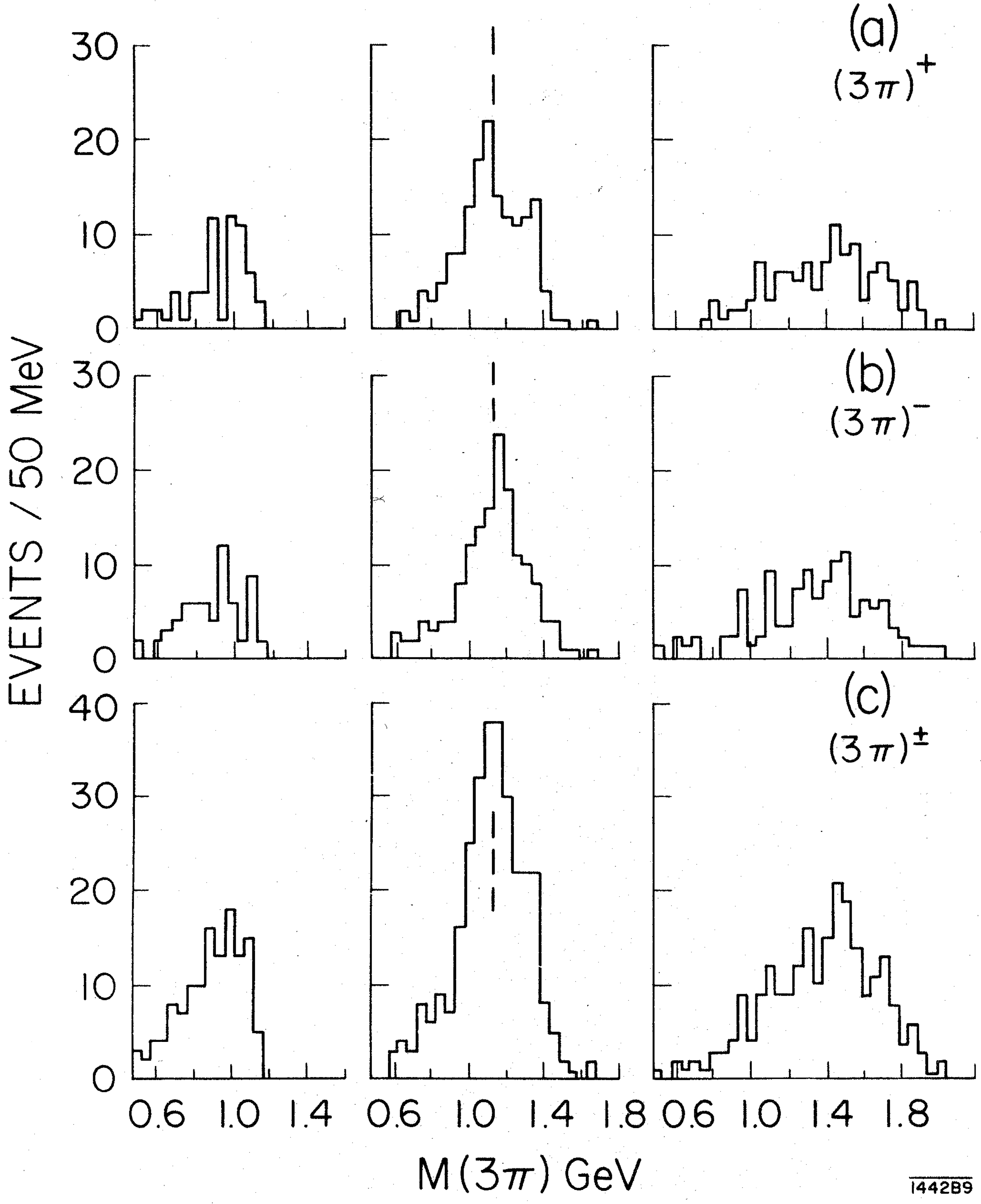
(a)
$(3\pi)^+$
(b)
$(3\pi)^-$
(c)
$(3\pi)^\pm$
EVENTS / 50 MeV
0
10
20
30
40
0.6
1.0
1.4
1.8
M(3π) GeV
1442B9

Fig. 7a, b, c

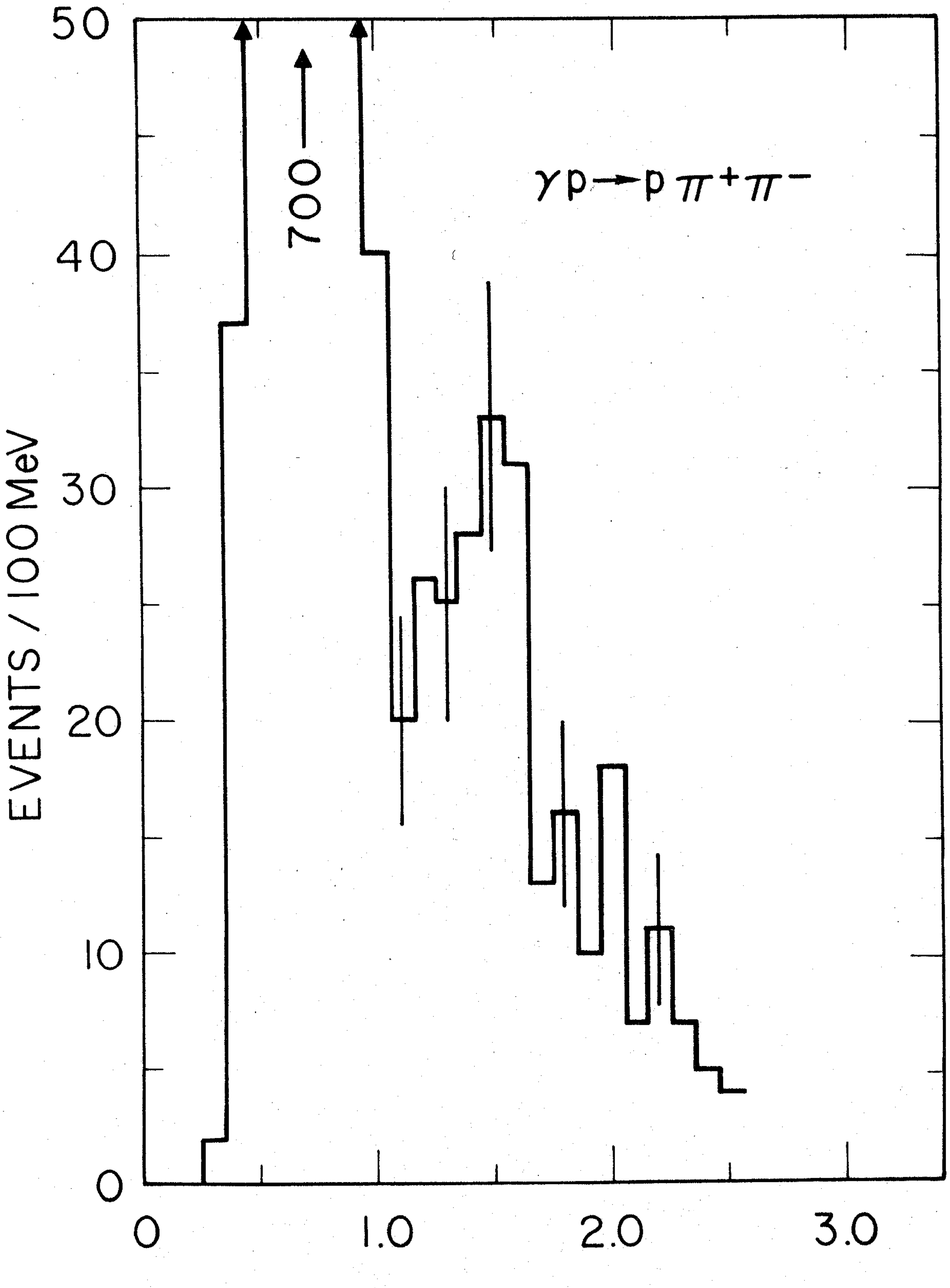

γp → pπ⁺π⁻
700
EVENTS / 100 MeV
M (π⁺π⁻) GeV
0
10
20
30
40
50
0
1.0
2.0
3.0
1442B7

Fig. 8

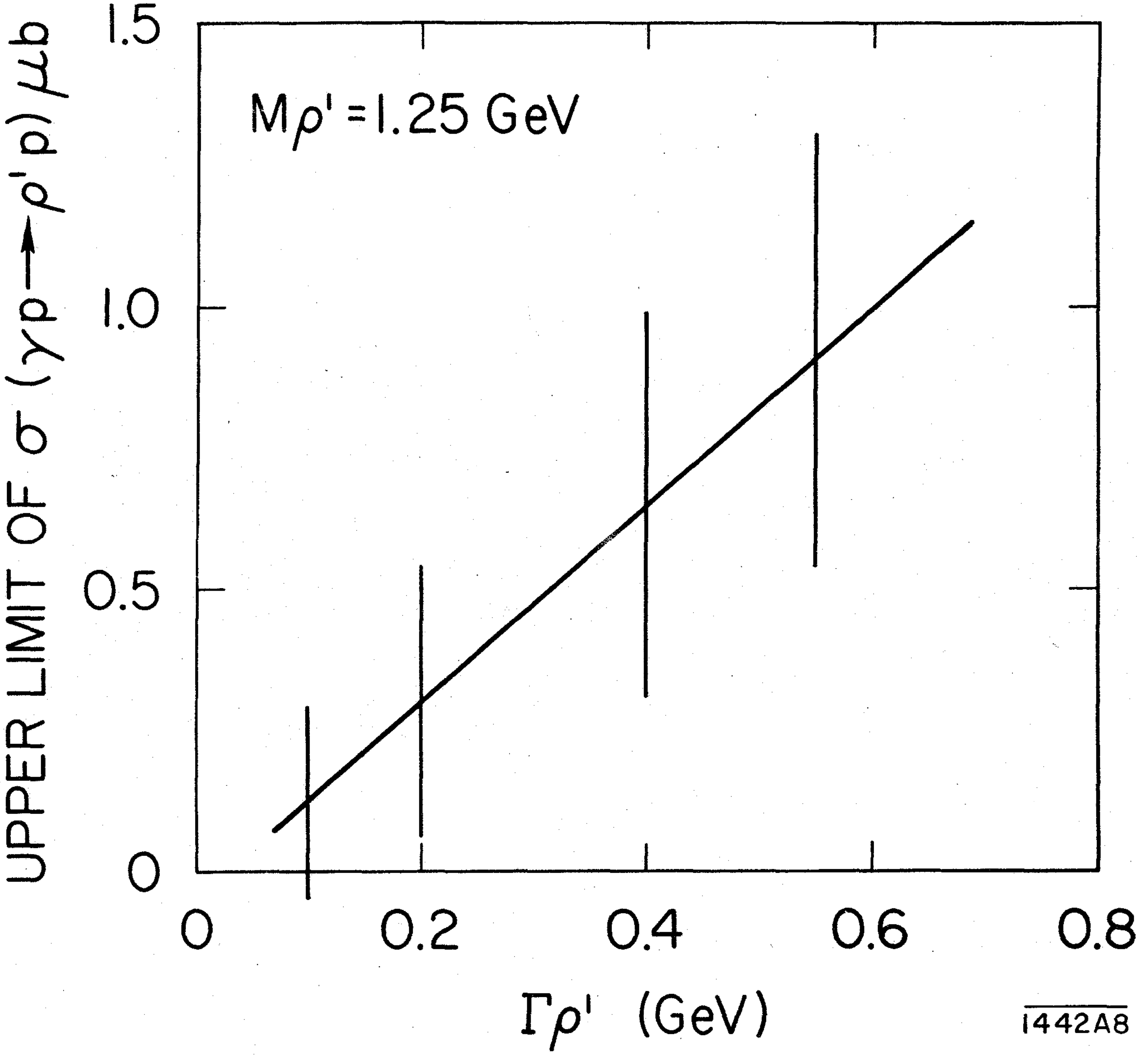
UPPER LIMIT OF σ (γp → ρ'p) μb
1.5
1.0
0.5
0
Mρ' = 1.25 GeV
0
0.2
0.4
0.6
0.8
Γρ' (GeV)
1442A8

Fig. 9